Title: DFT Study of Adsorption and Diffusion of Atomic Hydrogen on Metal Surfaces

Author: Elizabeth del V. Gómez Sebastián Amaya-Roncancio Lucía B. Avalle Daniel H. Linares M. Cecilia Gimenez

PII: S0169-4332(17)31335-1
DOI: http://dx.doi.org/doi:10.1016/j.apsusc.2017.05.032
Reference: APSUSC 35967

To appear in: *APSUSC*

Received date: 23-3-2017
Revised date: 28-4-2017
Accepted date: 3-5-2017

Please cite this article as: Elizabeth del V. Gómez, Sebastián Amaya-Roncancio, Lucía B. Avalle, Daniel H. Linares, M. Cecilia Gimenez, DFT Study of Adsorption and Diffusion of Atomic Hydrogen on Metal Surfaces, *<![CDATA[Applied Surface Science]]>* (2017), http://dx.doi.org/10.1016/j.apsusc.2017.05.032

DFT Study of Adsorption and Diffusion of Atomic Hydrogen on Metal Surfaces

Elizabeth del V. Gómez[(1)], Sebastián Amaya-Roncancio[(2)], Lucía B. Avalle[(1)], Daniel H. Linares[(2)] and M. Cecilia Gimenez[(1)] *
(1) IFEG, CONICET, FaMAF, UNC, Córdoba, Argentina.
(2) INFAP, CONICET, UNSL, San Luis, Argentina.

May 15, 2017

Abstract

An extensive study of adsorption and diffusion of hydrogen atoms on (100) surfaces of fcc Au, Cu, Ag and Pt was performed by means of DFT calculations. Bulk properties of those metals were calculated and compared with previous results. The adsorption distances and energies of the hydrogen atom on top, hollow and bridge sites of the (100) surfaces were calculated in order to elucidate preferential adsorption sites of hydrogen on each metal. All these calculations were done in conjunction with a study of charge distribution. Finally, diffusion of the H atom from the most stable adsorption site to the nearest neighbouring site was studied in order to obtain diffusion barrier and diffusion velocity values. The highest diffusion velocity was found to be $v = 6.44 \times 10^{11} s^{-1}$ for the case of Ag, whereas the lowest was $v = 1.13 \times 10^{7} s^{-1}$ for Au.

Keywords: DFT, adsorption, diffusion, surfaces.

*Corrresponding author. e-mail:cgimenez@famaf.unc.edu.ar

1 Introduction

As the study of adsorbed hydrogen on metal surfaces has long been a topic of interest for science and engineering, it has been investigated both through experimental [1, 2] and theoretical [3, 4] methods.

Its importance lies in the properties and current applications [5] of hydrogen, which is abundant, renewable and non-polluting. Given the scarcity of fossil fuels, hydrogen is considered as the energy source of the future [6, 7]. In this sense, fuel cells play an important role in obtaining and storing these energies, since they can generate electricity by electrochemically combining hydrogen and oxygen, without any combustion.

Fuel cells are normally made by metal surfaces which are used as catalysts where adsorption, diffusion and chemical reactions of the involved components occur [8, 9]. In this way, the interaction between hydrogen and metallic surfaces is an interesting and relevant subject to be studied [3, 10, 4].

Experimental study of hydrogen adsorption and diffusion on the surfaces of transition metals with a (100) orientation can be found in several reports.

Experimentally ordered hydrogen phases were measured as a function of temperature for different transition metals and the adsorption sites were determined [11, 12]. Lauhon et al studied diffusion of hydrogen atoms on $Cu(001)$ by STM measurements. The H atom diffusion was measured as a function of temperature and showed a transition from thermally activated diffusion to quantum tunneling at 60 K [13]. Dissociation, adsorption, and diffusion of hydrogen on a $Pd(111)$ surface have been studied within a $37 - 90K$ temperature range, where the diffusion parameters were determined from a statistical analysis [14]. For hydrogen vacancy diffusion in a $(1x1)$ phase a hopping rate of $4 \times 10^{-4} s^{-1}$ at $65K$ was obtained by these authors.

Although the present subject has been extensively studied regarding theoretical research, there are technical differences in all cases. We can mention unit cell size, coverage, slab thickness among other parameters that influence the obtained results. Systematic studies carried out in the last years [3, 4] show that the approximation level of the results depends to a considerable extent on the exchange-correlation functional used to investigate the faces of the metals studied.

Ferrin et al [3] have investigated diffusion of hydrogen from the surface to the bulk using the $PW91$ density functional [15], whereas Kristinsdóttir et al [4], have studied surface diffusion on several metals by means of RPBE [16]. In addition, the calculations performed with GGA-PBE functionals, have been widely accepted in the scientific community and have been extensively used in systems with periodic boundary conditions [17, 18, 19, 20, 21]. Even with the mentioned references, the fcc (100) surfaces of Au, Cu, Ag and Pt,

still present wide interest due to its application and future role in energy consumption of the population.

In the present work, we have carried out comprehensive calculations within the frame of the density functional theory (DFT), and we have employed the commonly used Perdew-Burke-Ernzerhof (PBE) version of the generalized gradient approximation (GGA), since there are a lot of tests that show that it gives total-energy-dependent properties in good agreement with experiment [22, 23, 24]. With this method we have calculated the adsorption energies of atomic hydrogen on the fcc (100) surfaces of Au, Cu, Ag and Pt. In addition, diffusion velocities were calculated in order to understand the microscopic mechanism of diffusion on surfaces.

Our main goal is to further understand the influence of several metal surfaces on the diffusion velocity of atomic hydrogen. This study has an important application for a deeper understanding of the basic mechanism involved in fuel cells hydrogen in the context of renewable energies.

2 Computational methods

All DFT calculations were done using the Quantum Espresso package [25]. The electron-ion interaction was described by Ultra-Soft pseudopotentials with scalar relativistic correction generated by Rappe-Rabe-Kaxiras-Joannopoulos method (RRKJUS) [26]. The generalized gradient approximation (GGA) for the exchange/correlation density functional PerdewBurkeErnzerhof (PBE) was used [27]. The chosen cutoff energies were 80 for Pt, 60 for Cu and 70 Ry for Ag and Au. The threshold for self-consistency was $1 \times 10^6\ eV$.

Brillouin zone integration was approximated using the MonkhorstPack scheme [28] with $12 \times 12 \times 12$ k-point sampling in bulk calculations and $4 \times 4 \times 1$ k-point sampling in slab calculations. The energy cutoff and k-grid points used in this work allow to calculate total energy with an error lower than $10^{-3} Ry$ as compared with larger grids and energy cutoffs (see Figs. S1 and S2 in the support information).

The calculated lattice parameters of Pt, Cu, Ag and Au were 4.00 $\mathring{A}$, 3.67 $\mathring{A}$, 4.16 $\mathring{A}$ and 4.18 $\mathring{A}$ respectively (see Fig. S3 in support information). All those values are consistent, have been compared with experimental ones which have been previously reported and are well explained in the next section.

The vacuum between the slabs was set at 10 $\mathring{A}$ thick along the [100] direction. The adsorption energies of hydrogen in different slab models are shown at Table ST1 (support information). A $p(2x2)$ supercell with five-metal layers was used (See Fig. 1). The chosen size is enough to describe

adsorption energy with and accuracy of 0.01 eV. The first three layers were fixed at the bulk position and the other two were allowed to relax describing the (100) surface where H is adsorbed. Hydrogen-adsorption energy is converged for a $p(2x2)$ model in good agreement with calculations of H adsorption on $Fe(100)$ performed by Amaya et al [19, 20, 21] and by Soresc u [29].

The geometry relaxation was done using BFGS quasi-Newton algorithm until the forces on each atom were less than 10^{-5} $eV/\mathring{A}$ and the energy difference of consecutive steps was less than 10^{-5} eV. Study of the minimum energy paths was undertaken using the Nudged Elastic Band Method (NEB) [30] and the local minima were found through the conjugate gradient (CG) technique. All molecular and density plots were made using the XCrySDen package [31].

3 Results and discussion

3.1 Bulk properties

Bulk properties were studied in order to corroborate the accuracy of the method employed in this work. Lattice parameters, bulk modulus and cohesion energies (or vaporization energy) were calculated for Pt, Cu, Ag and Au.

Table 1 shows the values obtained, all of which seem to be in good agreement with both experimental data [32] and other theoretical works reported [33, 24].

The lattice parameter for Pt, Cu, Ag and Au bulk was obtained by self-consistency calculations of the total energy whithin a certain range around the experimental value (with a variation step of $0.01\mathring{A}$) and finding the minimum of the curve (Table 1 and Figure S3 in supporting information).

In the case of the bulk modulus, an energy versus volume curve was fitted with the Murnaghan state equation [34].

The bulk modulus is defined by the following equation:

$$B_0 = -V\frac{\Delta P}{\Delta V} \tag{1}$$

where V represents the volume of the solid and P an external pressure. In practice, it was obtained by adjusting the energy data as a function of volume according to Murnaghan's equation of state [34]:

$$E(V) = E_0 + \frac{B_0 V}{B_0'}\left(\frac{(V_0/V)}{B_0'-1}+1\right) - \frac{B_0 V_0}{B_0'-1} \tag{2}$$

The latter relates the energy E of the unit with the volume V cell and with structural parameters such as the volume of the cell that minimizes the energy of the system, V_0, the Young modulus, B_0, B_0' and the minimum system energy E_0.

On the other hand, cohesion energy was calculated according to:

$$E_{coh} = E_{at} - E_{bulk}/N \tag{3}$$

where E_{at} is the energy of the atom isolated in vacuum and E_{bulk} denotes the energy of the crystal unit cell containing N atoms. According to this definition, a more positive value in the cohesion energy indicates stronger interatomic interactions (see Table 1).

3.2 Hydrogen adsorption

The adsorption energies and diffusion pathway were calculated for hydrogen atoms on (100) surfaces of representative metals: Au, Cu, Ag and Pt. First, the adsorption energies of the hydrogen atom on the three different adsorption sites (hollow, bridge and top) were calculated and the obtained values were compared with previous reports [3, 17, 18, 35, 36, 37, 38, 39, 40]. In some of that works, Moussounda et al [35] and Nave et al [17] have studied the adsorption energy for a single H atom and then for a single CH_3 on $Pt(100)$ in order to find the dissociation pathway of CH_4 on this surface. The results for the adsorption of H computed by them in reference are in good agreement with those obtained in the present work.

As the first step in the study of the mechanisms of H diffusion on the (100) surface of Pt, Cu, Ag and Au, it was necessary to calculate the adsorption energies of the hydrogen atom on the different sites already mentioned. The adsorption energies (E_{ads}) were calculated according to the following equation:

$$E_{ads} = E_{H/slab} - (E_{slab} + E_H) \tag{4}$$

where $E_{H/slab}$ is the energy of the whole system (hydrogen adsorbed on the surface), E_{slab} denotes the energy of the clean surface and E_H is the energy of an hydrogen atom in the vacuum. Both the energies and the equilibrium distances obtained are shown in Table 2.

According to the values in Table 2 it can be noticed that the bridge site proved to be the most favorable for H adsorption on the $Pt(100)$ surface. This is in agreement with previous studies [17, 35, 36], where this trend is reported.

The obtained energies were $-3.96eV$, $-3.74eV$ and $-3.62eV$ for bridge, top and hollow sites respectively. Meanwhile, the bond lengths were 1.02 $\mathring{A}$, 1.57 $\mathring{A}$ and 0.57 $\mathring{A}$, values that agree quite well with those reported by Nave et al. [17] for the same sites (1.06 $\mathring{A}$, 1.57 $\mathring{A}$ and 0.59 $\mathring{A}$). In the same way, the reported adsorption energies are in good agreement with the ones we obtained, in spite of the fact that four atomic layers were used in the previously mentioned work [17].

In the case of the $Cu(100)$ surface, energies of -3.42 eV and -3.27 eV were found for the hollow and bridge sites, respectively (see Table 2). It should be noted that hydrogen adsorbs only on these sites and not on top site. When a hydrogen atom is initially located on a top site, it relaxes to an adjacent hollow site during the geometry-optimization. However, the hollow site proved to be the most stable for adsorption of the atomic hydrogen in agreement with previous works [18, 3].

According to the results obtained, the most stable site for H adsorption on the $Ag(100)$ surface was the hollow site, whose energy value was -3.00 eV. Meanwhile, bridge and top sites were found to be less stable with energies of $-2.95eV$ and $-2.44eV$, respectively. Even though there are precedents of this trend [37, 38], Ferrin et al [3] and Eichler et al [39] reported the bridge site as the preferential one for H adsorption, although the energy difference between these sites was less than 0.06 eV. Particularly, in the present study, an energy difference of 0.05 eV was recorded for the aforementioned sites, but the hollow site was favored (see Table 2).

As regards the $Au(100)$ surface, only H adsorption on the bridge and top sites was considered, since the hydrogen atom in hollow position, tended to move to the adjacent bridge site during geometry optimization. This behavior had been previously observed by N'Dollo et al [40]. Thus, the lowest recorded energy was the one for the bridge site, with a value of -3.27 eV, resulting in the most stable site for adsorption. This behavior is in agreement with previous studies [3, 40]. On the other hand, the energy recorded on the top site was -2.87 eV.

The equilibrium distances for the most adsorptive sites are comparable in all cases with those reported by [3] who reported distances of 1.02 $\mathring{A}$ (bridge); 0.56 $\mathring{A}$ (hollow); 1.04 $\mathring{A}$ (hollow) and 0.93 $\mathring{A}$ (bridge) for Pt, Cu, Ag and Au respectively.

3.3 Charge distribution and LDOS of adsorbed hydrogen on metal surfaces

With the aim of understanding electron interaction of the adsorbed hydrogen with the several metal surfaces, we have evaluated the pseudo-difference of the electronic charge density for the adatom and each adsorption site of the studied metals. The pseudo-difference of the electronic charge density $\Delta\rho$ was calculated using Equation 5, as proposed by Dal Corso et al [26]:

$$\Delta\rho = \rho_{H/slab} - (\rho_{slab} + \rho_H) \tag{5}$$

where ρ is the electronic charge density and the subscripts $H/slab$, $slab$ and H refer to the hydrogen/slab, isolated slab and isolated hydrogen, respectively.

The pseudo charge electronic density calculations obtained from Equation 5 on each adsorption site, are shown in Figs. $2-5$, where the accumulation lobes of charge density are observed around H in each case with the metal surfaces. This fact reveals the covalent nature of the bonding with the metal atoms. Similarly, a depletion of charge density was observed on all metal surfaces studied, indicating that the surfaces are making up for the lack of electron density of the adsorbed hydrogen and shown the behavior of the several metals as catalysts. The electronic density results are complemented by calculation of the local density of states (LDOS) for the atoms involved in the preferential adsorption sites for each case.

Although the resulting charge density calculations are similar for all the metals studied, the mentioned electron density transfer strongly depends on the adsorption site. Accordingly, in the case of $H/Pt(100)$, where the bridge site was found to be the preferential adsorption site, the accumulation of electron density is higher than that of the same atom adsorbed on the hollow and top sites (see Fig. 2). In the case of adsorption on the bridge site, an accumulation of charge density can be observed near the H atom. This fact is supported by the LDOS calculation, where the states of Pt present a shift towards the state of the adsorbed H in comparison with the clean metal (Fig. 2d).

In the case of $H/Cu(100)$, the calculations present an accumulation of charge density around the hydrogen adsorbed on the hollow and bridge sites, and a depletion of charge between the first and the second layer of the Cu surface, as shown in Fig. 3. Observation of the depletion agrees with the nature of the metal surfaces as a charge reservoir. The main depletion between the two adsorption sites is observed in hollow which agrees with the adsorption energy and the LDOS calculations. The states of Cu are modified by the presence of H indicating a covalent nature of adsorption (Fig. 3c).

For the $H/Ag(100)$ system, charge depletion generated on the Ag surface as an effect of the presence of the adsorbed hydrogen, was observed in a larger amount than for the other studied metals, as it can be seen in Fig. 4. In this metal the hollow and bridge sites present similar adsorption energies, and the accumulation lobes are located between H and Ag atoms (Figs. 4a and b). In LDOS calculation (Fig. 4d) the behavior of states is similar to the previous cases in the sense that the states of the metal shift towards the state of H.

Finally, for the $H/Au(100)$ system, hydrogen presents a charge accumulation/depletion similar to that of the previous cases on its preferential adsorption site. In the case of hydrogen adsorbed on the bridge site for $Au(100)$, even when depletion is easily observable, it does not present the charge density as the previous cases (see Fig. 5a). For hydrogen adsorbed on the top site of $Au(100)$, an accumulation of charge around the adsorbed hydrogen can be seen as shown in Fig. 5b. This fact suggests that adsorbed hydrogen can easily diffuse through these sites. The accumulation lobes shown on the bridge site (Fig. 5a) explain the difference between the adsorption energies in the different sites. The LDOS calculation (Fig. 5c) support the preference of the H atom to be adsorbed in bridge site, where the d-states of Au are strongly modified by the presence of the hydrogen atom.

3.4 Difussion Pathway for Hydrogen on metal surfaces

In order to clarify the diffusion pathway of the atomic hydrogen on the analyzed surfaces $Pt(100)$, $Cu(100)$, $Ag(100)$ and $Au(100)$, the minimum energy path of diffusion was studied on each metal surface. For this purpose, the most stable site for hydrogen adsorption was taken into account, and calculations were carried out from this site to the most stable near neighboring site. As can be observed in Table 2, the most stable adsorption sites are bridge for the case of Au and Pt and hollow for the case of Cu and Ag (the ones that present the minimum adsorption energy). The path for the diffusion between the neighbouring most stable adsorption sites occurs through the second most stable adsorption site (top for the two first cases and brigde for the two last cases).

For the case of $Pt(100)$, hydrogen diffusion was performed from a bridge site to the next bridge site as shown in Fig. 6. Here, the atomic hydrogen adsorbed on the bridge site (Fig. 6a), is promoted to the neighbor top site, as shown in Fig. 6b. The energy required for hydrogen diffusion from a bridge to an adjacent top site was estimated at $0.20eV$ (see Table 3). From this top site, where an adsorption state was observed (Fig. 6b), hydrogen is promoted to the near bridge (Fig. 6c) with a diffusion barrier calculated at $0.02eV$ (see

Fig. 6 and Table 3).

In the case of $Cu(100)$, diffusion was performed from a hollow site to the near hollow site as shown in Fig. 7*a*. Here, the minimum energy path for diffusion is found to passing through the adjacent bridge site as depicted in Fig. 7*b*. Here, the bridge site does not show an adsorption behavior and the energy required for diffusion in the present case was $0.18eV$ (see Table 3).

For hydrogen diffusion on $Ag(100)$ (Fig. 8), the initial configuration adopted was hydrogen adsorbed on a hollow site. Even if the behavior observed here is similar to that of Cu, the diffusion energy for the Ag system was calculated in $0.10eV$ as shown in Table 3 and Fig. 8. In this case hydrogen diffusion presents its highest value on the bridge site (Fig. 8*b* and Table 3).

For $Au(100)$, the diffusion pathway of adsorbed hydrogen presents a diffusion barrier calculated at $0.40eV$ (see Fig. 9 and Table 3). Both the initial and final configuration obtained in our calculations are bridge sites since these are the most stable adsorption sites. The value of diffusion velocity was calculated passing through a top site and it is consistent with our previous calculations of adsorption sites.

In the present section, we can observe the energy of the diffusion barrier of atomic hydrogen calculated for the metals studied to go from $0.10eV$ to $0.40eV$. These values show that hydrogen diffusion is relevant to the studied metals and that it is viable under experimental conditions as reported in [14].

3.5 Calculation of Diffusion Velocities of Hydrogen on Metal Surfaces

For the calculation of diffusion rates, the vibrational frequencies were estimated at the starting point, and the theory of absolute velocities was used based on the formula:

$$v = \nu \times exp(-E_a/(k_B T)) \tag{6}$$

where ν is the vibrational frequency, E_a denotes the activation energy (i.e. the difference between the maximum and the minimum), k_B is the Boltzmann constant and T is the temperature (considered in this case as $T = 300K$). In order to calculate the vibrational frequency, some points were added in the reaction path, assuming that it is symmetric around the minimum and the curve was fitted around it with a parabola. The elastic spring constant was obtained from the coefficient of the quadratic term , assuming a harmonic movement, and then the frequency was calculated as:

$$\nu = \frac{1}{2\Pi} \times \sqrt{\frac{k}{m_H}} \tag{7}$$

where k is the elastic spring constant and m_H denotes the atomic mass of hydrogen.

Figure 10 shows the diffusion velocity of the hydrogen atom as a function of temperature for the four metals studied. For calculating velocity as a function of temperature, the formula 6 and the activation frequencies and energies of Table 3 were used. As it can be observed, the velocity is kept at relatively low values up to a certain temperature threshold value, where it abruptly rises. Taking as a criterion that speed exceeds the value of $1 \times 10^7 s^{-1}$ the threshold temperatures found are: $T = 300K$ for Au, $T = 160K$ for Pt, $T = 140K$ for Cu and $T = 80K$ for Ag .

4 Conclusions

The present work provides important insights into hydrogen diffusion on metal surfaces, where this topic has a wide use nowadays as catalysts of fuel cells energy production. DFT calculations were done with the aim of understanding microscopic diffusion velocities of the hydrogen atom on the (100) surfaces of Pt, Cu, Ag and Au.

Some bulk properties of the fcc Pt, Cu, Ag and Au were previously calculated and compared with those reported in the references. The adsorption energies of the hydrogen atom on the different adsorption sites of the (100) surfaces was calculated, and it was found that the most stable adsorption sites were hollow for Ag and Cu and bridge for Au and Pt. The pseudo charge difference calculated for each the systems studied shows that in all cases hydrogen takes charge from the surfaces generating a strong covalent interaction, but in the same line, electron interaction allows hydrogen to move on metal surfaces in each case.

The diffusion studied through calculation of the minimum energy paths on the several metal surfaces reveals that the diffusion barriers on the mentioned metal surfaces are $0.20eV$, $0.18eV$, $0.10eV$ and 0.40 eV for Pt, Cu, Ag and Au respectively. The obtained results make us conclude that the high adsorption energy of the hydrogen atoms keeps hydrogen on the metal surfaces but does not affect the mobility of the adsorbed atom through the surface.

The absolute rate theory was employed to calculate diffusion velocities for the hydrogen atom from one adsorbing site to the near neighbor site. It was found that at $T = 300K$ the diffusion rate was calculated to be $1.13 \times 10^7 s^{-1}$ for $H/Au(100)$, $2.31 \times 10^{10} s^{-1}$ for $H/Pt(100)$, $4.93 \times 10^{10} s^{-1}$ for $H/Cu(100)$

and $6.44 \times 10^{11} s^{-1}$ for $H/Ag(100)$. Finally, it can be concluded that the hydrogen atom diffuses faster on Ag, with a velocity one order of magnitude greater than that on Pt and Cu, and four orders of magnitude greater than that on Au.

5 ACKNOWLEDGMENTS

The authors thank support from CONICET (Argentina) and Secyt (U.N.C., Córdoba, Argentina). The calculations were carried out using the Verseo cluster located at Departamento de Química Computacional, INFIQC, Facultad de Ciencias Químicas, U.N.C., Córdoba, Argentina.

References

[1] N. Pentland, J. O'M. Bockris, and E. Sheldon *Hydrogen Evolution Reaction on Copper, Gold, Molybdenum, Palladium, Rhodium, and Iron: Mechanism and Measurement Technique under High Purity Conditions.* J. Electrochem. Soc., 104(3) (1957) 182-194.

[2] N.M. Marković, B.N. Grgur, and P.N. Ross. *Temperature-Dependent Hydrogen Electrochemistry on Platinum Low-Index Single-Crystal Surfaces in Acid Solutions.* J. Phys. Chem. B, 101(27) (1997) 5405-5413.

[3] Peter Ferrin, Shampa Kandoia, Anand Udaykumar Nilekara, and Manos Mavrikakisa. *Hydrogen adsorption, absorption and diffusion on and in transition metal surfaces: A DFT study.* Surface Science, 606(7-8) (2012) 679-689.

[4] Lilja Kristinsdóttir, and Egill Skúlason. *A systematic DFT study of hydrogen diffusion on transition metal surfaces.* Surface Science, 606(17-18) (2012) 1400-1404.

[5] *Hydrogen Effects in Catalysis: Fundamentals and Practical Applications.* edited by Z. Paál, P.G. Menon (1988).

[6] P. P. Edwards, V. L. Kuznetsov, W. I. F. David and N. P. Brandon. *Hydrogen and fuel cells: Towards a sustainable energy future.* Energy Policy 36 (2008) 4356 - 4362.

[7] H. J. Neef. *International overview of hydrogen and fuel cell research.* Energy 34 (2009) 327 - 333.

[8] T. Jacob. *The Mechanism of Forming H_2O from H_2 and O_2 over a Pt Catalyst via Direct Oxygen Reduction.* Fuel Cells 06 (2006) Nro. 3 - 4, 159 - 181.

[9] M. T. M. Koper, R. A. van Santen. *Interaction of H, O and OH with metal surfaces.* Journal of Electroanalytical Chemistry 472 (1999) 126 - 136.

[10] Axel Gross. *Hydrogen on metal surfaces: Forever young.* Surface Science 606 (2012) 690 - 691.

[11] Stipe B.C., Rezaei M.A., and Ho W. J. Chem. Phys. (1997) 107, 6443.

[12] Stipe B.C., Rezaei M.A., and Ho W. *Atomistic studies of O 2 dissociation on Pt (111) induced by photons, electrons, and by heating.* J. Chem. Phys. (1998) Science, 280, 1732.

[13] LJ Lauhon, W Ho. *Direct Observation of the Quantum Tunneling of Single Hydrogen Atoms with a Scanning Tunneling Microscope.* Physical review letters, 85(21), 4566 (2000).

[14] Mitsui, T., Rose, M. K., Fomin, E., Ogletree, D. F., & Salmeron, M. *Hydrogen adsorption and diffusion on Pd(111).* Surface science, 540(1), 5-11 (2003).

[15] John P. Perdew, J. A. Chevary, S. H. Vosko, Koblar A. Jackson, Mark R. Pederson, D. J. Singh, and Carlos Fiolhais. *Atoms, molecules, solids, and surfaces: Applications of the generalized gradient approximation for exchange and correlation.* Physical Review B, 46(11) (1992) 6671 - 6687.

[16] B. Hammer, L. B. Hansen, and J. K. Nørskov. *Improved adsorption energetics within density-functional theory using revised Perdew-Burke-Ernzerhof functionals.* Physical Review B, 59(11) (1999) 7413-7421.

[17] Sven Nave, Ashwani Kumar Tiwari, and Bret Jackson. *Methane dissociation and adsorpton on Ni(111), Pt(111), Ni(100), Pt(100), and Pt(110)-(1x2): Energetic study.* The Journal of Chemical Physics, 132(5) (2010) 054705.

[18] Xian-Yong Pang, Li-Qin Xue, and Gui-Chang Wang. *Adsorption of Atoms on Cu Surfaces: A Density Functional Theory Study.* Langmuir, 23(9) (2007) 4910 - 4917.

[19] Amaya-Roncancio, S., Linares, D.H., Duarte, H.A., Lener, G. and Sapag, K. *Effect of Hydrogen in Adsorption and Direct Dissociation of CO on Fe (100) Surface: A DFT Study.* American Journal of Analytical Chemistry, 6 (2015)-

[20] S. Amaya-Roncancio, D.H. Linares, K. Sapag, M.I. Rojas. *Influence of coadsorbed H in CO dissociation and Conformation on Fe(1 0 0): A DFT study.* Applied Surface Science 346 (2015) 438442.

[21] Sebastiaán Amaya-Roncancio, Daniel H. Linares, Hélio A. Duarte, and Karim Sapag. *DFT Study of Hydrogen-Assisted Dissociation of CO by HCO, COH and HCOH Formation on Fe(100)* J. Phys. Chem. C (2016) 120, 1083010837.

[22] Stefan Kurth, John P. Perdew and Peter Blaha. *Molecular and Solid-State Tests of Density Functional Approximations: LSD, GGAs, and Meta-GGAs*. International Journal of Quantum Chemistry, Vol. 75 (1999), 889 - 909.

[23] Viktor N. Staroverov, Gustavo E. Scuseria, Jianmin Tao and John P. Perdew. *Tests of a ladder of density functionals for bulk solids and surfaces*. Physical Review B, 69 (2004) 075102.

[24] Patanachai Janthon, Sergey M. Kozlov, Francesc Viñes, Jumras Limtrakul, and Francesc Illas. *Establishing the Accuracy of Broadly Used Density Functionals in Describing Bulk Properties of Transition Metals*. Journal of Chemical Theory and Computation, 9(3) (2013) 1631 - 1640.

[25] Paolo Giannozzi, Stefano Baroni,Nicola Bonini, Matteo Calandra, Roberto Car, Carlo Cavazzoni, Davide Ceresoli,Guido L. Chiarotti, Matteo Cococcioni, Ismaila Dabo, Andrea Dal Corso, Stefano de Gironcoli, Stefano Fabris, Guido Fratesi, Ralph Gebauer, Uwe Gerstmann, Christos Gougoussis, Anton Kokalj,Michele Lazzeri, Layla Martin-Samos, Nicola Marzari, Francesco Mauri, Riccardo Mazzarello, Stefano Paolini, Alfredo Pasquarello,Lorenzo Paulatto, Carlo Sbraccia, Sandro Scandolo, Gabriele Sclauzero, Ari P. Seitsonen, Alexander Smogunov, Paolo Umari, and Renata M Wentzcovitch. *QUANTUM ESPRESSO: a modular and open-source software project for quantum simulations of materials*. Journal of Physics: Condensed Matter, 21(39) (2009) 395502.

[26] Andrea Dal Corso. *H.pbe-rrkjus.UPF, Pt.pbe-nd-rrkjus.UPF, Cu.pbe-d-rrkjus.UPF, Ag.pbe-d-rrkjus.UPF, Au.pbe-nd-rrkjus.UPF*. http://www.quantum-espresso.org

[27] John P. Perdew, Kieron Burke,and Matthias Ernzerhof. *Generalized Gradient Approximation Made Simple*. Physical Review Letters, 77(18) (1996) 3865 - 3868.

[28] M. Methfessel, and A. T. Paxton. *High-precision sampling for Brillouin-zone integration in metals*. Physical Review B, 40 (6) (1989) 3616 - 3621.

[29] Dan C. Sorescu. *First principles calculations of the adsorption and diffusion of hydrogen on Fe(1 0 0) surface and in the bulk*. Catalysis Today Volume 105, Issue 1, 15 July 2005, Pages 4465.

[30] Graeme Henkelman, Blas P. Uberuaga, and Hannes Jónsson. *Climbing Image Nudged Elastic Band Method for Finding Saddle Points and Min-*

imum Energy Paths. The Journal of Chemical Physics, 113(22) (2000) 9901 - 9904.

[31] Anton Kokalj *Graphics and Graphical User Interfaces as Tools in Simulations of Matter at the Atomic Scale*. Computational Materials Science, 28(2) (2003) 155-168.

[32] Charles Kittel. *Introduction to Solid State Physics*, 8th ed. John Wiley and Sons, Inc.: New York,2005.

[33] Philipp Haas, Fabien Tran, and Peter Blaha. *Calculation of the lattice constant of solids with semilocal functionals*. Physical Review B, 79(8) (2009) 085104.

[34] F. D.Murnaghan. *The Compressibility of Media Under Extreme Pressures*. Proceedings of the National Academy of Sciences of the United States of America, 30(9) (1944) 244 - 247.

[35] P.S. Moussounda, M.F. Haroun, G. Rakotovelo, P. Légaré. *A theoretical study of CH_4 dissociation on Pt(100) surface*. Surface Science, 601(18) (2007) 3697 - 3701.

[36] Farida Saad, Mourad Zemirlin, Mouloud Benakki, and Said Bouarab. *Ab-initio study of the coadsorption of Li and H on Pt(001), Pt(110) and Pt(111) surfaces*. Physica B:Condensed Matter, 407(4) (2012) 698 - 704.

[37] C. Qin, and J. L. Whitten. *Adsorption of O, H, OH, and H_2O on Ag(100)*. The Journal of Physical Chemistry B, 109(18) (2005) 8852 - 8856.

[38] Sung Chul Jung, and Myung Ho Kang. *Effect of hydrogen on the surface relaxation of Pd(100), Rh(100), and Ag(100)*. Physical Review B, 72(20) (2005) 205419.

[39] A. Eichler, J. Hafner, and G. Kresse. *Hydrogen Adsorption on the (100) Surfaces of Rhodium, Palladium and Silver*. Surface Review and Letters, 4(6) (1997) 1297 - 1303.

[40] M. Ndollo, P. S. Moussounda, T. Dintzer, and F. Garin. *A Density Functional Theory Study of Methoxy and Atomic Hydrogen Chemisorption on Au(100) Surface*. Journal of Modern Physics, 4(3A) (2013) 409 - 417.

Figure Captions:

Figure 1. Schematic representation of the slab used in this work. a) Top view showing the three characteristic adsorption sites (top, bridge and hollow). b) Side view of the slab, showing the five layers employed.

Figure 2. Charge density isosurface for the hydrogen atom adsorbed on $Pt(100)$ on: (a) hollow, (b) bridge and (c) top sites, for a density of 0.002 $eV/\mathring{A}^3$. Regions with charge accumulation are shown in red, while those with charge depletion are shown in blue. d) Ldos of H atom adsorbed on a bridge site of $Pt(100)$. 1s-orbital for H (black), d-orbitals of the clean metal surface (red) and the complete system (green).

Figure 3. Charge density isosurface for the hydrogen atom adsorbed on $Cu(100)$: (a) hollow and (b) bridge sites, for a density of 0.002 $eV/\mathring{A}^3$. Regions with charge accumulation are shown in red, while those with charge depletion are shown in blue. c) Ldos of H atom adsorbed on a hollow site of $Cu(100)$. 1s-orbital for H (black), d-orbitals of the clean metal surface (red) and the complete system (green).

Figure 4. Charge density isosurface for the hydrogen atom adsorbed on $Ag(100)$: (a) hollow, (b) bridge and (c) top sites, for a density of 0.002 $eV/\mathring{A}^3$. The regions with charge accumulation are shown in red, while those with charge depletion are shown in blue. d) Ldos of H atom adsorbed on a hollow site of $Ag(100)$. 1s-orbital for H (black), d-orbitals of the clean metal surface (red) and the complete system (green).

Figure 5. Charge density isosurface for the hydrogen atom adsorbed on $Au(100)$ on: (a) bridge and (b) top sites, for a density of0.002 $eV/\mathring{A}^3$. The regions with charge accumulation are shown in red, while those with charge depletion are shown in blue. c) Ldos of H atom adsorbed on a bridge site of $Au(100)$. 1s-orbital for H (black), d-orbitals of the clean metal surface (red) and the complete system (green).

Figure 6. a) Energy of the system as a function of the diffusion pathway

for a H atom on a $Pt(100)$ surface, from a bridge site to another bridge site passing through a top site. b) initial state, c) transition state and d) final state. Points, calculated states from NEB. Solid line, extrapolation of the energy surface.

Figure 7. a) Energy of the system as a function of the diffusion pathway for a H atom on a $Cu(100)$ surface, from a hollow site to another hollow site passing through a bridge site. b) initial state, c) transition state and d) final state. Points, calculated states from NEB. Solid line, extrapolation of the energy surface.

Figure 8. a) Energy of the system as a function of the diffusion pathway for a H atom on a $Ag(100)$ surface, from a hollow site to another hollow site passing through a bridge site. b) initial state, c) transition state and d) final state Points, calculated states from NEB. Solid line, extrapolation of the energy surface.

Figure 9. a) Energy of the system as a function of the diffusion pathway for a H atom on a $Au(100)$ surface, from a bridge site to another bridge site passing through a top site. b) initial state, c) transition state and d) final state. Points, calculated states from NEB. Solid line, extrapolation of the energy surface.

Figure 10. Diffusion velocity as a function of the temperature for a H atom on (100) surfaces of the four studied metals (Ag, Cu, Pt, and Au). The velocity was calculated between adjacent (more stable) adsorption sites.

6 Tables

Metal	Property	Calculations		Exp.c
		Actual	Previous	
Pt	$A_0(\mathring{A})$	4.00	3.985a	3.92
	B_0 (GPa)	238.7	250.9 b	278.3
	E_{coh} (eV)	5.71	5.50 b	5.84
Cu	$A_0(\mathring{A})$	3.67	3.632 a	3.61
	B_0 (GPa)	126.3	146.9 b	137
	E_{coh} (eV)	3.46	3.48 b	3.49
Ag	$A_0(\mathring{A})$	4.16	4.152 a	4.09
	B_0 (GPa)	89.6	83.3 b	100.7
	E_{coh} (eV)	2.61	2.49 b	2.95
Au	$A_0(\mathring{A})$	4.18	4.154 a	4.08
	B_0 (GPa)	133.1	138.4 b	173.2
	E_{coh} (eV)	3.07	2.99 b	3.81

[a] Referencia [33].
[b] Referencia [24].
[c] Referencia [32].

Table 1: Structural parameters obtained in the present study, compared to the experimental values [32] and those obtained by Hass et al [33] and Janthon et al [24].

	$E_{ads}(eV)$			d_{H-Sup} $(\mathring{A})$		
Metal	Hollow	Bridge	Top	Hollow	Bridge	Top
Pt	-3.62	-3.96	-3.74	0.57	1.02	1.57
Cu	-3.42	-3.27	*	0.45	1.03	*
Ag	-3.00	-2.95	-2.44	0.33	1.03	1.67
Au	*	-3.27	-2.87	*	0.89	1.60

Table 2: H adsorption energies on different adsorption sites (E_{ads}) and distances from H to the surface plane (d_{H-Sup}).

System	ν (s^{-1})	$E_a(eV)$	v (s^{-1})
H/Pt	6.60x10^{13}	0.21	2.31x10^{10}
H/Cu	3.99x10^{13}	0.17	4.93x10^{10}
H/Ag	2.35x10^{13}	0.09	6.44x10^{11}
H/Au	5.41x10^{13}	0.40	1.13x10^{07}

Table 3: Vibrational frequencies around the minimum (ν); Activation energies (E_a) and diffusion rates (v) for the systems under study, for a temperature of $T = 300K$.

A study of adsorption and diffusion of hydrogen atoms on (100) surfaces of fcc Au, Cu, Ag and Pt, which was performed by means of DFT calculations.

Bulk properties of those metals were calculated and compared with previous results.

The distances and energies of the hydrogen atom on the different adsorption sites of the (100) surfaces were calculated.

Velocity values for the diffusion of hydrogen on the different surfaces were calculated.

Figure

Click here to download Figure: fig01.pdf

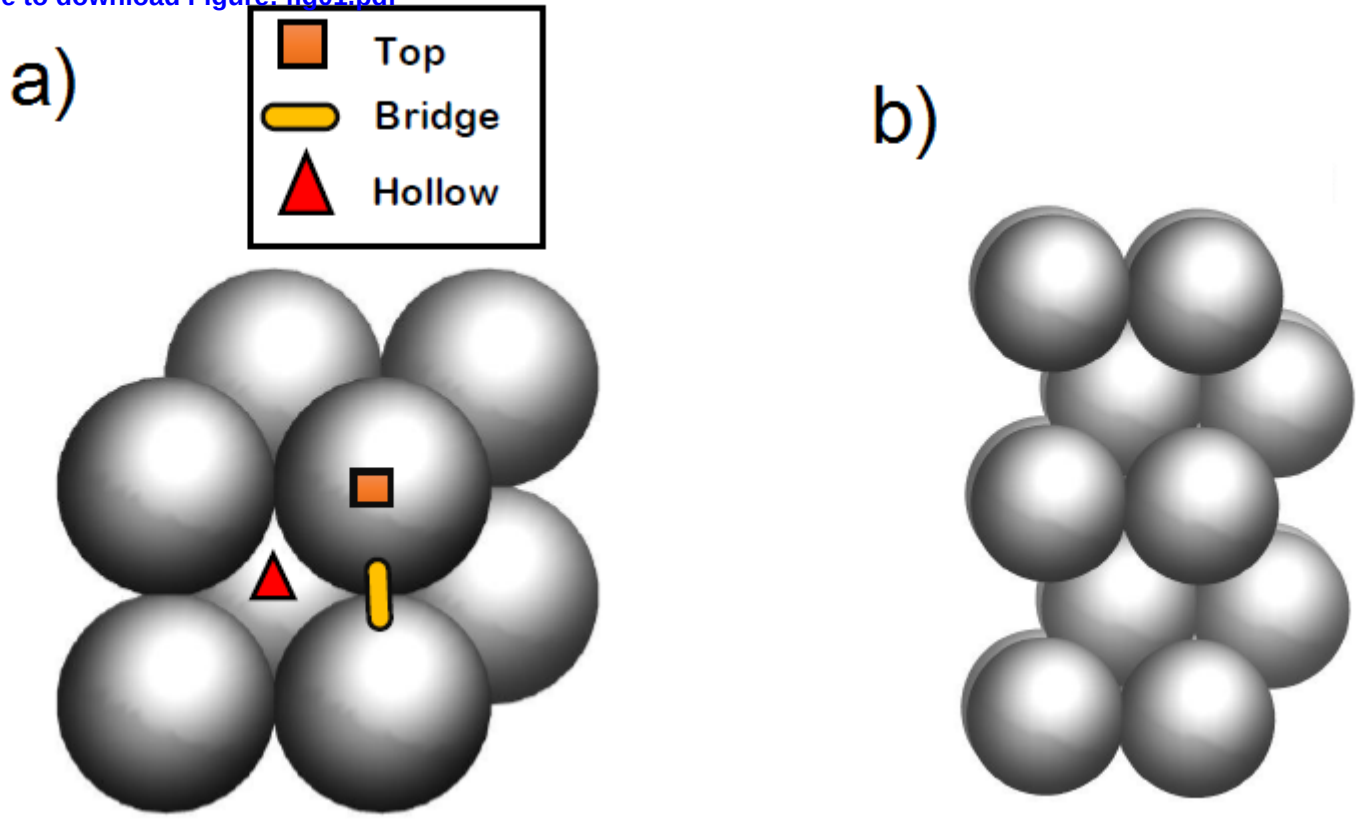

Figure
Click here to download Figure: fig02-HPt.pdf

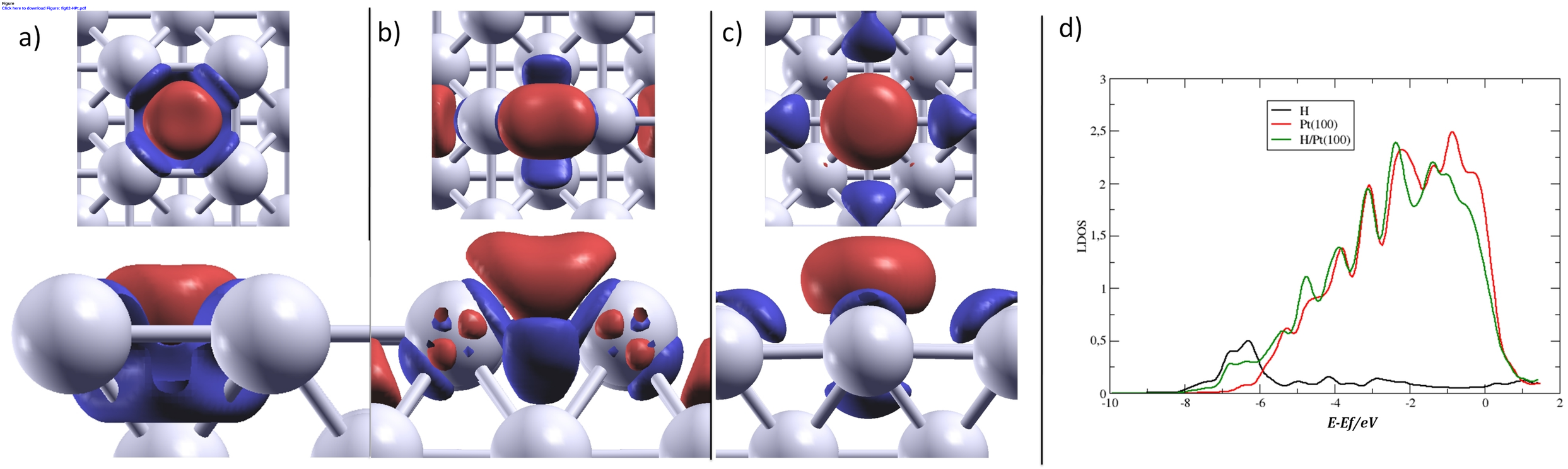

Figure
Click here to download Figure: fig03-HCu.pdf

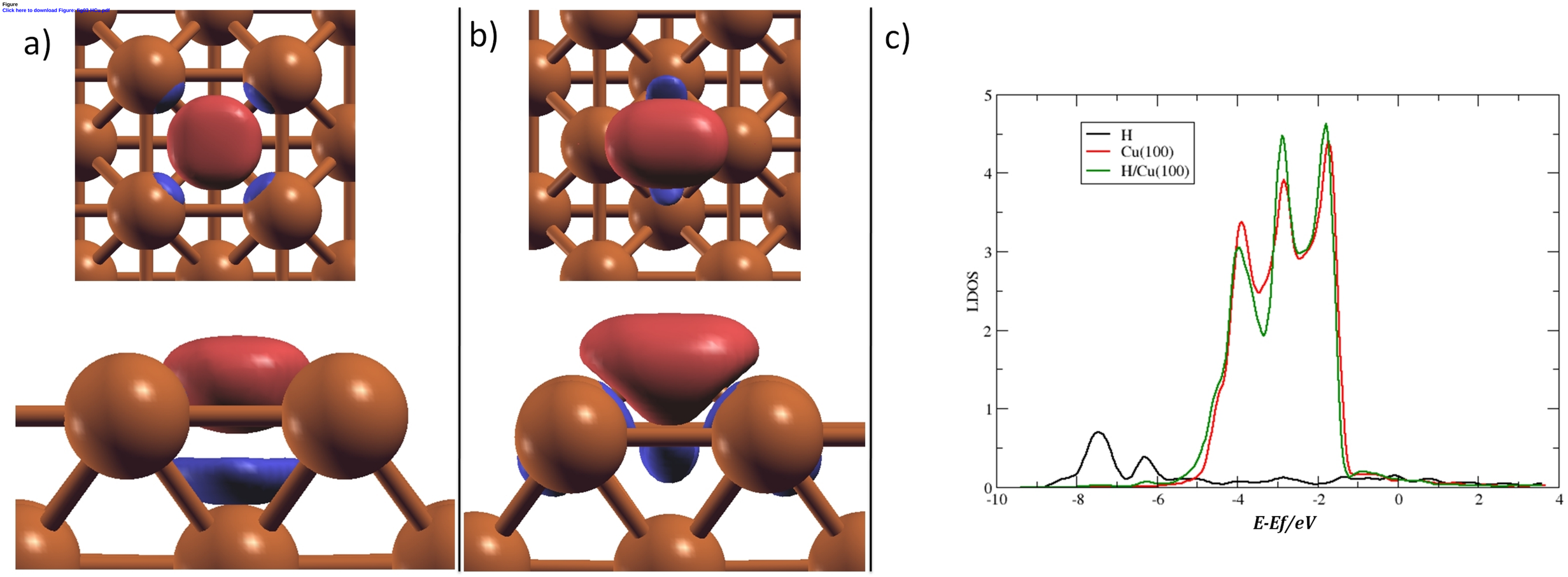

Figure
Click here to download Figure: fig04-HAg.pdf

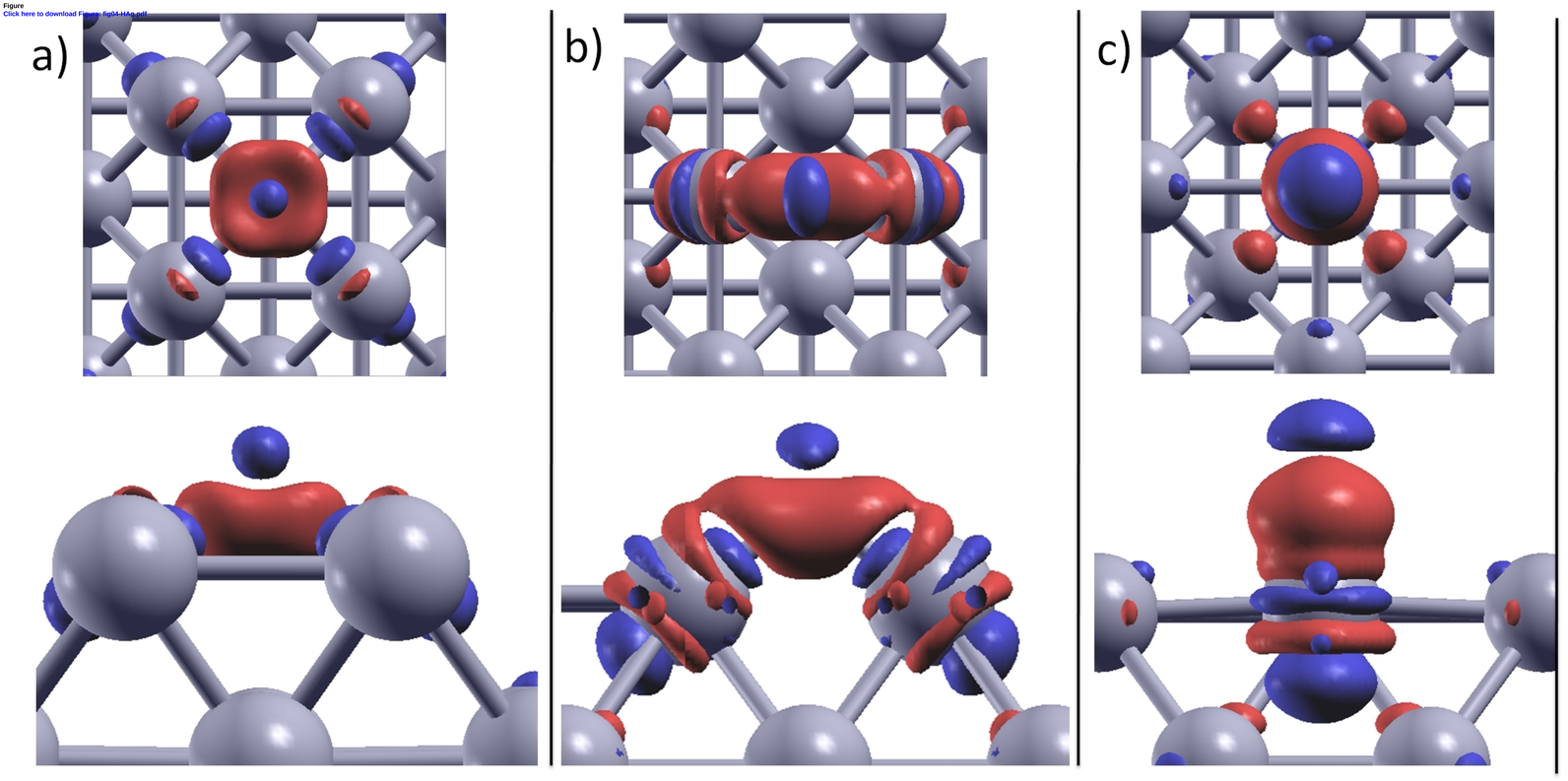

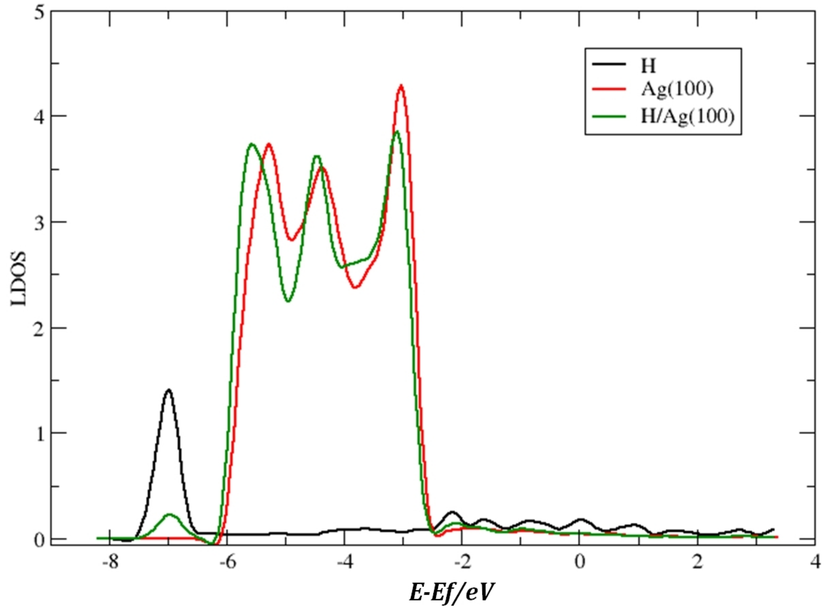

Figure
Click here to download Figure: fig05-HAu.pdf

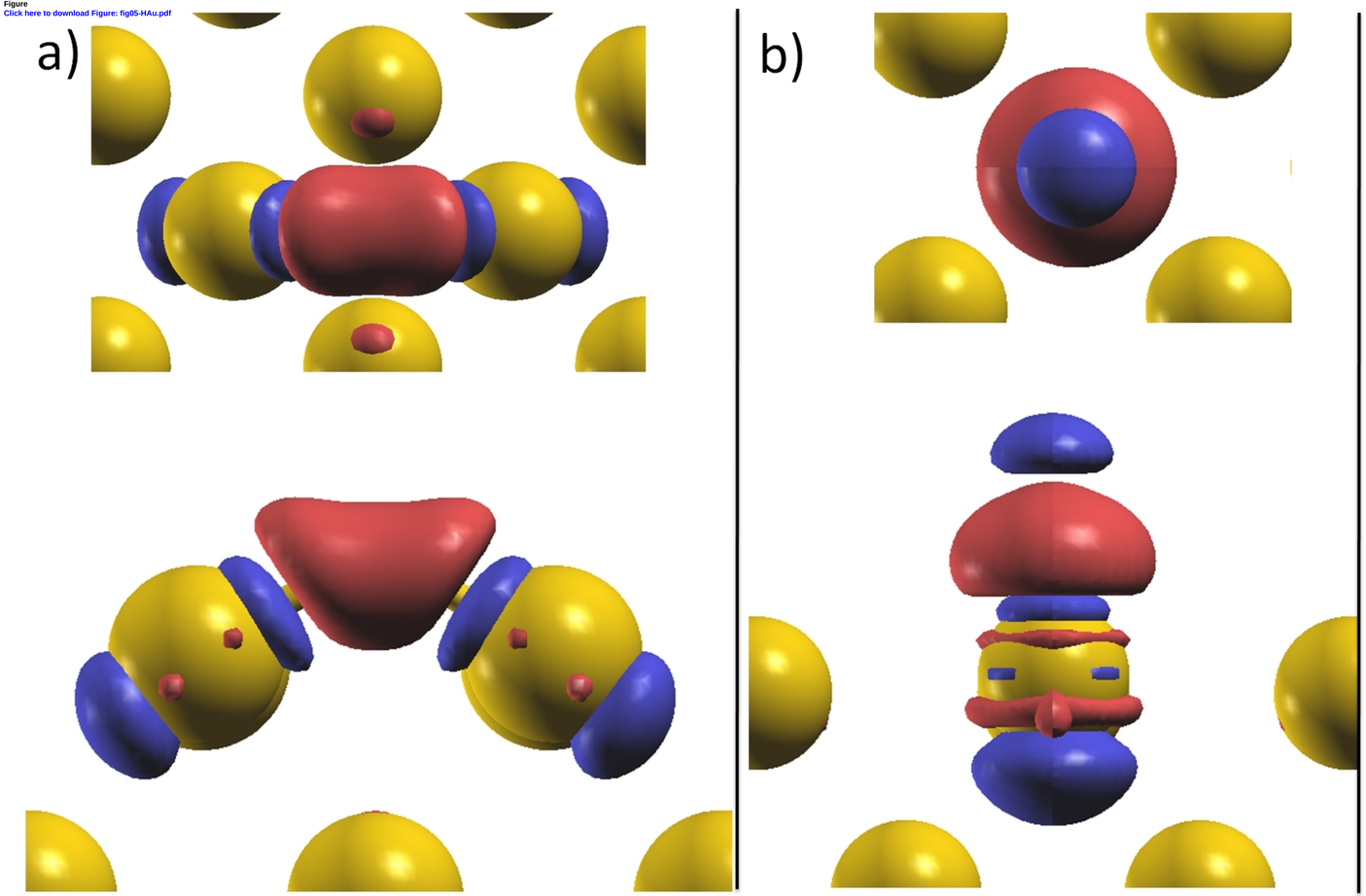

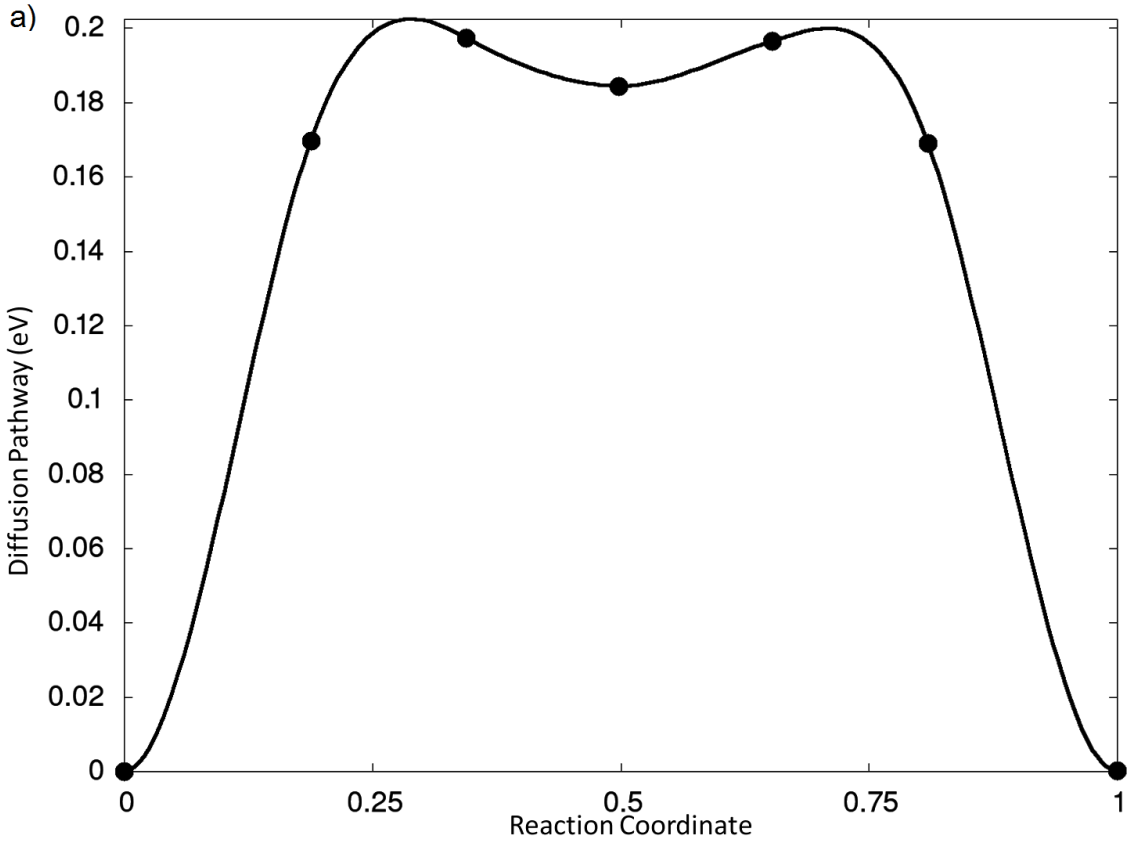

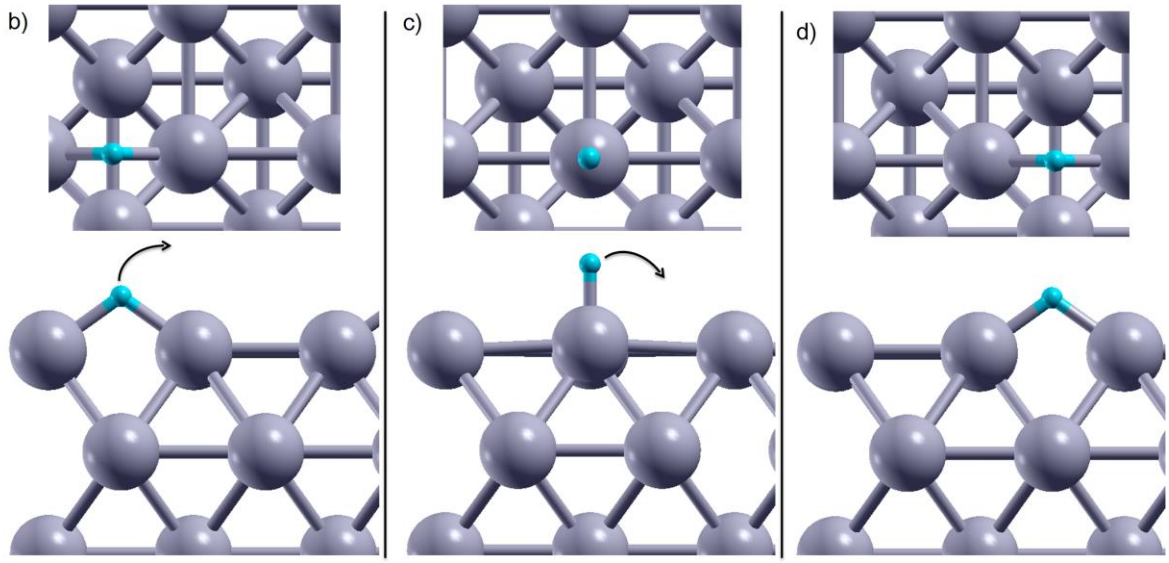

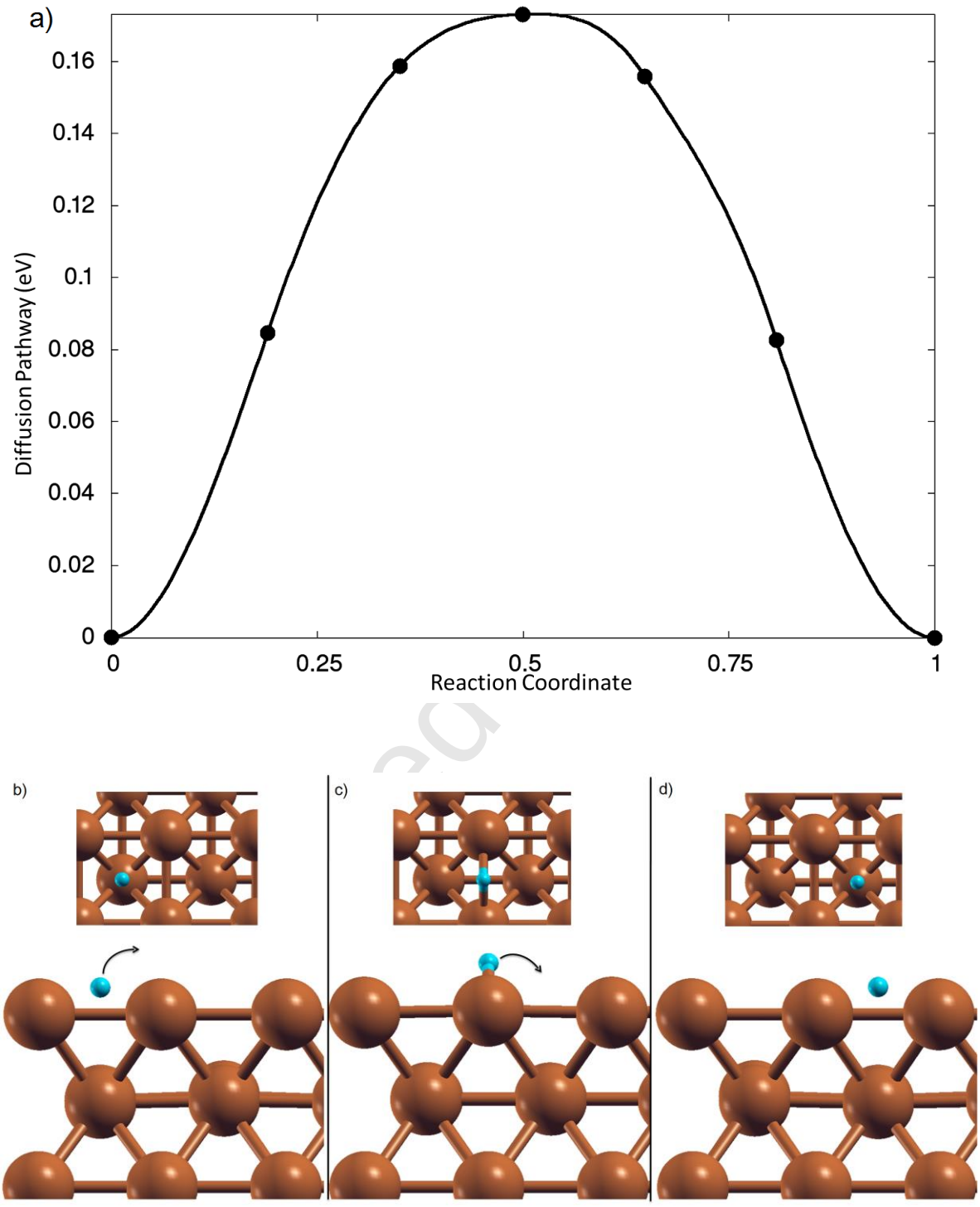

Figure
Click here to download Figure: fig08-NEB-Ag.pdf

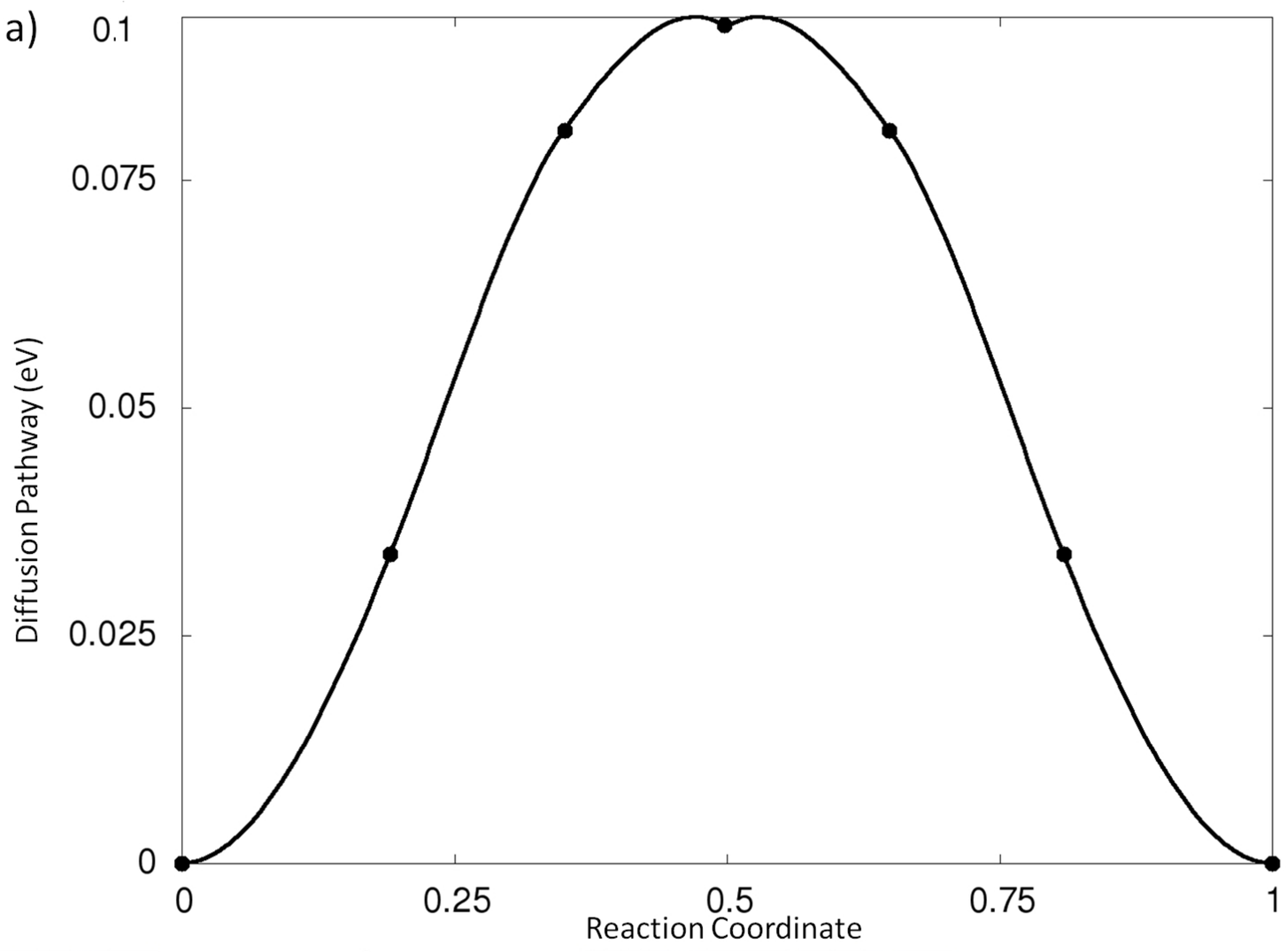

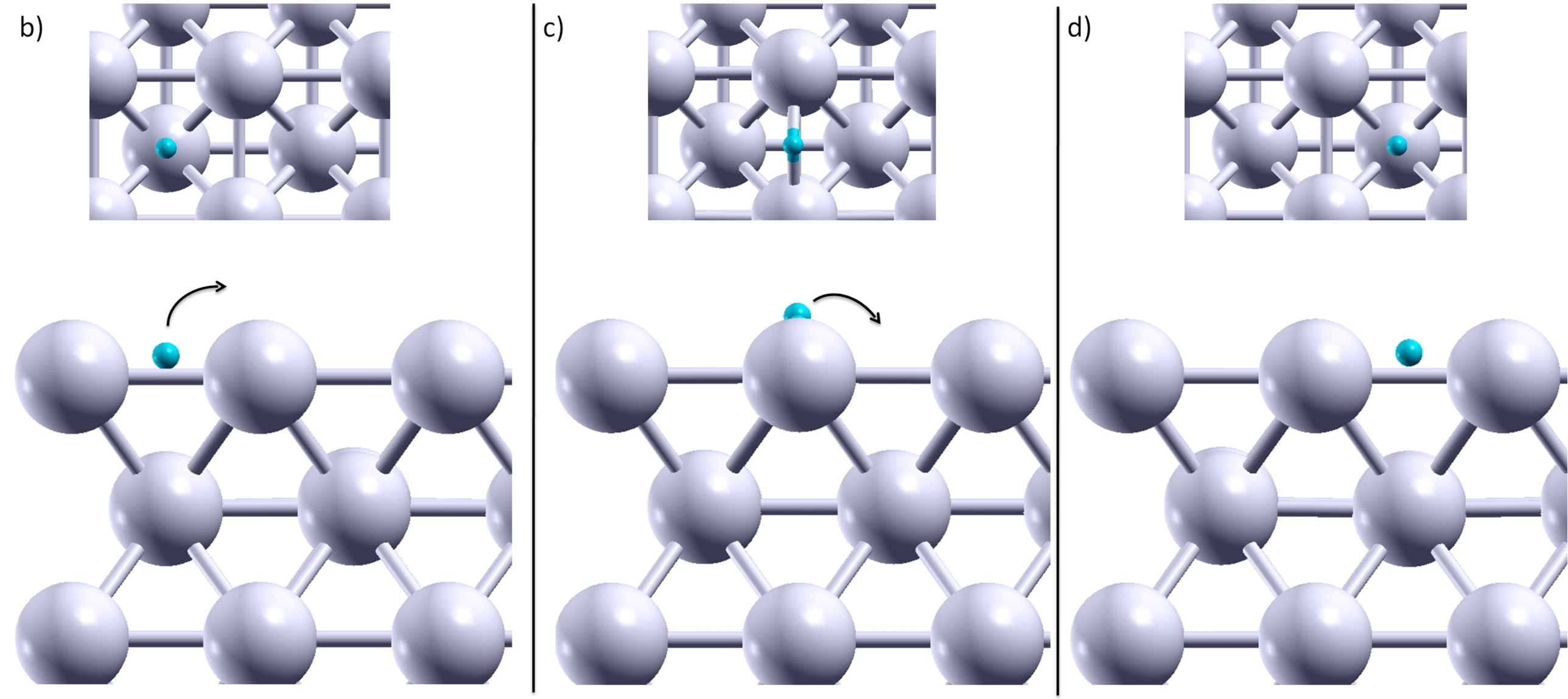

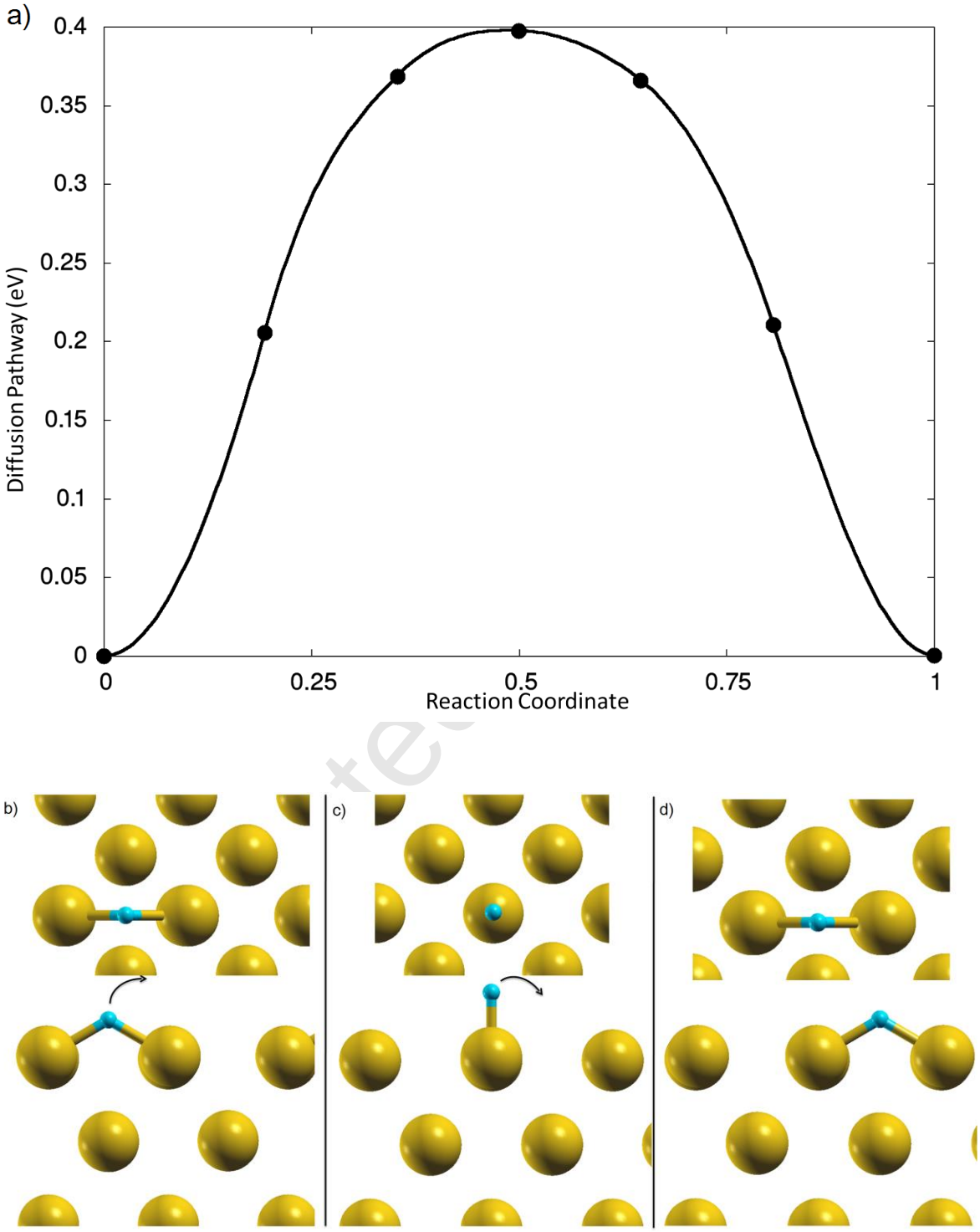

Figure
Click here to download Figure: fig10-vel.pdf